DOI 10.1007/978-3-319-05041-6_13
Reprinted from the *Journal of Nanoparticle Research*, DOI 10.1007/s11051-012-0881-x

RESEARCH PAPER

Arsenic removal by magnetic nanocrystalline barium hexaferrite

Hasmukh A. Patel · Jeehye Byun · Cafer T. Yavuz

Received: 13 November 2011 / Accepted: 18 April 2012 / Published online: 28 June 2012

Abstract Nanoscale magnetite (Fe_3O_4) (<15 nm) is known to remove arsenic efficiently but is very difficult to separate or require high magnetic fields to separate out from the waste water after treatment. Anisotropic hexagonal ferrite ($BaFe_{12}O_{19}$, BHF) is a well-known permanent magnet (i.e., fridge magnets) and attractive due to its low cost in making large quantities. BHF offers a viable alternative to magnetite nanocrystals for arsenic removal since it features surfaces similar to iron oxides but with much enhanced magnetism. Herein, we employ BHF nanocrystalline materials for the first time in arsenic removal from wastewater. Our results show better (75 %) arsenic removal than magnetite of the similar sizes. The BHF nanoparticles, 6.06 ± 0.52 nm synthesized by thermolysis method at 320 °C do not show hexagonal phase, however, subsequent annealing at 750 °C produced pure hexagonal BHF in >200 nm assemblies. By using BHF, we demonstrate that nanoparticle removal is more efficient and fixed bed type cartridge applications are more possible.

Keywords Hexaferrites · Nanoparticles · Magnetic · Arsenic removal · Adsorption · Magnetite · Sustainable development · Water resources

Special Issue Editors: Mamadou Diallo, Neil Fromer, Myung S. Jhon

This article is part of the Topical Collection on Nanotechnology for Sustainable Development

H. A. Patel · J. Byun · C. T. Yavuz (✉)
Graduate School of EEWS, Korea Advanced Institute of Science and Technology (KAIST), Daejeon 305-701, Republic of Korea
e-mail: yavuz@kaist.ac.kr
URL: http://yavuz.kaist.ac.kr/

Introduction

Arsenic is one of the most toxic contaminants found in the environment and has been recognized as a toxic element for centuries. Arsenic contamination has become a worldwide epidemic, especially in developing countries where a significant percentage of the population depends on groundwater for drinking. Elevated concentrations of arsenic in groundwater are found in many countries such as India, Bangladesh, Vietnam, and Chile (Mohan and Pittman 2007; Acharyya et al. 1999; Sharma and Sohn 2009).

The toxicity of arsenic to human health ranges from skin lesions to cancer of the brain, liver, kidney, and stomach. A wide range of arsenic toxicity has been determined that depends on arsenic speciation. Generally inorganic arsenic species are more toxic than organic forms to living organisms, including humans and other animals. To minimize the health impact of arsenic, the United States Environmental Protection Agency adopted a new maximum contaminant level of 10 μg/L in drinking water on January 22, 2001 (Pena et al. 2005). Arsenic is naturally present in groundwater

in the forms of arsenite (AsO_3^{3-}) and arsenate (AsO_4^{3-}). These anions resemble phosphite (HPO_3^{2-}) and phosphate (PO_4^{3-}) ions, and it is this similarity that is the dominant source of their toxicity: arsenite and arsenate block ATP → ADP conversions by permanently replacing phosphate groups (Yavuz et al. 2010).

Among methods developed to remove the arsenic from contaminated water such as coagulation and flocculation, precipitation, ion exchange, and membrane filtration, adsorption is the most widely used because it is simple, cost-effective, and sludge-free. The effectiveness of adsorption primarily depends on the characteristics of the adsorbent; therefore, there has been considerable interest in identifying the proper adsorbents for arsenic removal. So far, many adsorbents such as zirconium based gel (Biswas et al. 2008), agricultural residue (Ranjan et al. 2009; Shipley et al. 2011), iron modified bauxite (Bhakat et al. 2006), porous materials (Li et al. 2007), modified carbon black (Borah et al. 2009) and polymeric materials (Cumbal et al. 2003; Lim et al. 2009) have been developed for the removal of arsenic. Magnetically activated adsorbents, especially magnetite nanoparticles have been extensively studied as a promising adsorptive material and offer new opportunities for enhanced separation in complex environmental systems due to their durability, resistance to oxidation, less susceptibility to fouling by natural organic matters, high isoelectric point, high surface area, and selectivity for arsenic species (Beker et al. 2010; Tang et al. 2011; Yavuz et al. 2006; Yean et al. 2005; Mayo et al. 2007; Yavuz et al. 2010; Yavuz et al. 2009; Yean et al. 2005). As(III) is more mobile and toxic (25–60 times) than As(V). This elevated toxicity is due to its preferential reaction with sulfhydryl groups in mammalian enzymes (Pena et al. 2005). As(III) is also known to prefer neutral species (H_3AsO_3) at conventional water pH ranges i.e., pH 6–8, unlike As(V), making it more difficult to remove as shown in Table 1.

Nanoscale magnetic iron oxides show great promise in applications such as magnetic data storage, water treatment, ferrofluids, medical imaging, drug targeting, and catalysis, because of their inexpensive, non-toxic and high temperature stability (Kwon and Hyeon 2008; Zeng et al. 2002; Yavuz et al. 2006; Zhao et al. 2011). Among magnetic iron oxides, the hexagonal ferrites, especially barium hexaferrite ($BaFe_{12}O_{19}$, BHF) receive the widest commercial interest due to their availability and high magnetocrystalline anisotropy (1.7 T), featuring high coercivity, remanent magnetization and ferromagnetic resonance (Tucek et al. 2010). The enhanced magnetism identifies BHF as an improved magnetic adsorbent since its parent iron oxide, magnetite shows significant arsenic removal (Yavuz et al. 2006).

Table 1 Effect of pH on the ionic state of As(III) and As(V)

For As(III)	
$H_3AsO_3 \rightarrow H_2AsO_3^- + H^+$	$pK_{a1} = 9.22$
$H_2AsO_3^- \rightarrow HAsO_3^{2-} + H^+$	$pK_{a2} = 12.13$
$HAsO_3^{2-} \rightarrow AsO_3^{3-} + H^+$	$pK_{a3} = 13.40$
For As(V)	
$H_3AsO_4 \rightarrow H_2AsO_4^- + H^+$	$pK_{a1} = 2.2$
$H_2AsO_4^- \rightarrow HAsO_4^{2-} + H^+$	$pK_{a2} = 6.97$
$HAsO_4^{2-} \rightarrow AsO_4^{3-} + H^+$	$pK_{a3} = 11.53$

Though there have been a number of attempts to synthesize nanoparticles of BHF by various techniques (Junliang et al. 2010), such as thermolysis, reverse micro-emulsion, co-participation, hydrothermal process, sol–gel route, none resulted in highly monodisperse nanocrystals. On the contrary, monodisperse transition metal-based ferrite nanoparticles, $MnFe_2O_4$, $CoFe_2O_4$, $NiFe_2O_4$, $FeFe_2O_4$, are well documented, where high temperature aging of metal–surfactant complexes are commonly employed (Hyeon et al. 2002; Bao et al. 2007).

In this brief communication, we attempt to utilize barium hexaferrites for the removal of As(III) from contaminated waters. To the best of our knowledge this is the first report in BHF-mediated arsenic removal. By using BHF, we demonstrate that nanoparticle removal is more efficient and fixed bed type cartridge applications are more probable. BHFs were synthesized by a successful thermolysis of ferric hydroxide, barium hydroxide, oleic acid in 1-octadecene and subsequent annealing.

Experimental

Materials

1-Octadecene (technical grade, 90 %) and oleic acid (99 %) were obtained from Sigma-Aldrich, USA. Iron(III) hydroxide (90 %), barium hydroxide octahydrate (97 %), *n*-hexane (99.5 %), magnetite (50–100 nm) and ethyl alcohol (99.5 %) were

obtained from SAMCHUN, South Korea. As(III) standard solution (1,000 mg/L) was purchased from Fluka.

Synthesis of BHF ($BaFe_{12}O_{19}$)

0.979 g (11 mmol) Iron (III) hydroxide and 0.31 g (0.96 mmol) barium hydroxide octahydrate were mixed and powdered using mortar-pestle. This mixture, 11.3 g (40 mmol) oleic acid and 25 g 1-octadecene were transferred into a 100 mL three-neck round bottom flask equipped with condenser, magnetic stirrer, thermocouple, and heating mantle. The reaction mixture was heated under vigorous stirring at 5 °C/min up to 320 °C and kept at this temperature for 90 min under dinitrogen environment. Subsequently, the resulted black mixture was cooled down to room temperature and washed several times with ethyl alcohol. The wax-like black material was then dispersed into *n*-hexane for further characterization and designated as BHF. The BHF nanoparticles were annealed at 550 and 750 °C at a heating rate of 5 °C/min and the temperature were maintained for 2 h. The annealed samples are designated as BHF-550 and BHF-750.

As(III) adsorption and desorption study

Arsenic adsorption experiments were performed with 0.1, 0.5, 1, 5, and 10 mg/L of As(III) solutions, prepared in an electrolyte solution containing 0.01 M NaCl, 0.01 M tris(hydroxymethylamino)methane buffer, and 0.01 M NaN_3 at pH 8. All experiments were performed in batches with 10 mg of sample/L of solution. Equilibrium time was 24 h, with constant tumbling. The solution was separated from BHF by a strong magnet and aliquots were analyzed for As(III) concentration by ICP-AES and ICP-MS. The data of arsenic adsorption was analyzed by Langmuir and Freundlich isotherm models. Desorption was conducted as batch experiments in aqueous alkaline solution of sodium hydroxide (pH 13). After adsorption cycle, BHF-750 was separated, dispersed in 10 mL of alkaline solution and allowed for tumbling for 24 h at room temperature. The particles were magnetically removed and solutions were acidified by dilute nitric acid for arsenic measurement.

Characterization

TEM images were collected by Field Emission Transmission Electron Microscope (FE-TEM, 200 kV, Tecnai F20). Samples for TEM investigations were prepared by putting an aliquot of *n*-hexane solution of nanoparticles onto an amorphous carbon substrate supported on a copper grid. The excess liquid was then removed, and the grid was allowed to dry at room temperature. In order to investigate the morphology of annealed BHF particles, sample loaded on Si(100) wafer were characterized by scanning electron microscopy (SEM, Magellan400). X-ray diffraction analyses were carried out using Micro-area X-ray diffractometer (Rigaku, D/MAX-2500). The quantitative analyses of Iron, barium, and arsenic were measured by inductively coupled plasma atomic emission spectroscopy (ICP-AES) or inductively coupled plasma atomic mass spectroscopy (ICP-MS). BHF was digested in concentrated nitric acid for elemental analysis.

Results and discussion

The powder XRD patterns (Fig. 1) of the BHF synthesized at different temperatures clearly reveal that hexaferrites phase is formed after annealing at 750 °C. The diffraction peaks at 2 θ value of 30.34°, 32.31°, 34.17°, 37.15°, 56.8°, and 63.16° correspond to diffraction planes (110), (107), (114), (203), (2011) and (2200), respectively. These patterns can be ascribed to hexagonal $BaFe_{12}O_{19}$ phase (JCPDS # 84-0757). The BHF-750 is in single phase with hexagonal structure without showing any detectable impurities. The as-made BHF contains Fe_2O_3 and Fe_3O_4 as major phases (JCPDS # 86-0550 and 79-0417) therefore it was annealed at 550 and 750 °C. Annealing below 750 °C does not result in hexagonal phase, as evident from XRD patterns. The crystallite size of BHF-750 has been calculated from the Debye–Scherrer formula (Hessien et al. 2008; Patel et al. 2008), using the full width at half maximum (FWHM) value of the most intense peak (114) in the X-ray patterns using,

$$\text{Crystallite size} = K\lambda/W\cos\theta$$

where $W = W_b - W_s$ and W_b is the broadened profile width of experimental sample and W_s is the standard profile width of reference silica sample.

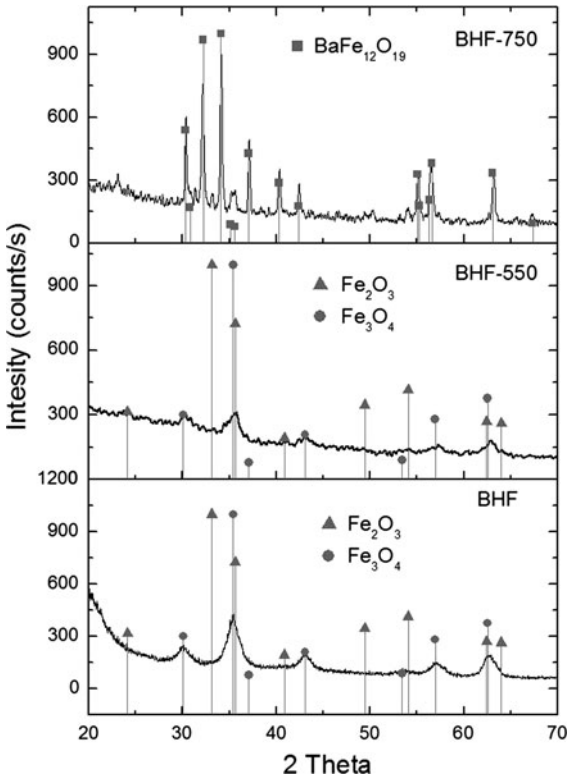

Fig. 1 X-ray diffraction patterns of as-synthesized BHF and annealed BHF-550, BFH-750

The crystallite size of BHF-750 is 61.7 nm, however, the particle size of BHF-750 varies from 200–550 nm.

TEM image (Fig. 2a) showed particles of spherical shapes, uniform in size with an average particle diameter of 6.06 ± 0.52 nm for BHF. The particle sizes are consistent throughout the sample as observed from TEM images. The chemical compositions measured by ICP-AES show Fe/Ba molar ratio is 11.6, fit well with the theoretical ratio in corresponding barium and strontium hexaferrite compounds. Although Fe/Ba = 11.6 is observed in BHF, XRD pattern suggest that there is no evidence of hexagonal phase formation. This implies that barium is not integrated and it requires higher temperature for inclusion of barium into hexagonal phase. The annealing of BHF nanoparticles distorted size, which resulted agglomeration and size of BHF-750 increased substantially. The SEM image reveals agglomerated particles of BHF-750 (Fig. 2b) with particle size varies from 200–550 nm.

We use As(III) as a typical contaminant to investigate the potential application of BHF in environment pollution control. As one of the most toxic and carcinogenic chemical elements, arsenic has been recorded as a priority issue by the World Health Organization (WHO). Today, perhaps more than 100 million people in India, Bangladesh, Vietnam, Nepal, China, and possibly other countries are drinking water with arsenic concentrations up to 100 times the WHO guideline of 10 μg/L. Batch experiments were conducted to determine As(III) removal efficiency for BHF-750. In batch experiment, 10 mg/L of BHF was interacted with As(III) solutions of 0.1, 0.5, 1, 5, and 10 mg/L. Figure 3 shows the As(III) removal with respect to various concentration. Initially, adsorption of As(III) occurred rapidly up to As(III) concentration of 1 mg/L. The arsenic removal efficiency at this point is 0.88 mg/g. After this, saturation begins, indicates equilibrium of As(III) was started and attained complete saturation at 10 mg/L where arsenic removal efficiency is 2.37 mg/g.

The isotherm models of Langmuir and Freundlich were used to fit the experimental adsorption equilibrium data of arsenic on BHF-750 (Zhao et al. 2010; Mayo et al. 2007). Adsorption isotherms, which are the presentation of the amount of solute adsorbed per unit of adsorbent as a function of equilibrium concentration in solution at constant temperature, were also studied. The Langmuir isotherm is valid for single-layer adsorption. It is based on the assumption that all the adsorption sites have equal affinity for molecules of the adsorbate and there is no transmigration of the adsorbate in the plane of the surface. Langmuir isotherm is presented as,

$$q_e = \frac{q_m K_L C_e}{1 + K_L C_e}$$

The Freundlich equation deals with physico-chemical adsorption on heterogenous surfaces (indicates the adsorptive capacity or loading factor) and is presented as,

$$q_e = K_F C_e^{1/n}$$

where C_e (mg/L) is the concentration of arsenic at equilibrium, K_L (L/mg), and q_m (mg/g) are the Langmuir constants related to the energy of adsorption and maximum capacity, respectively; K_F ($mg^{1-(1/n)}\ L^{1/n}\ g^{-1}$) and 1/n are the Freundlich constants

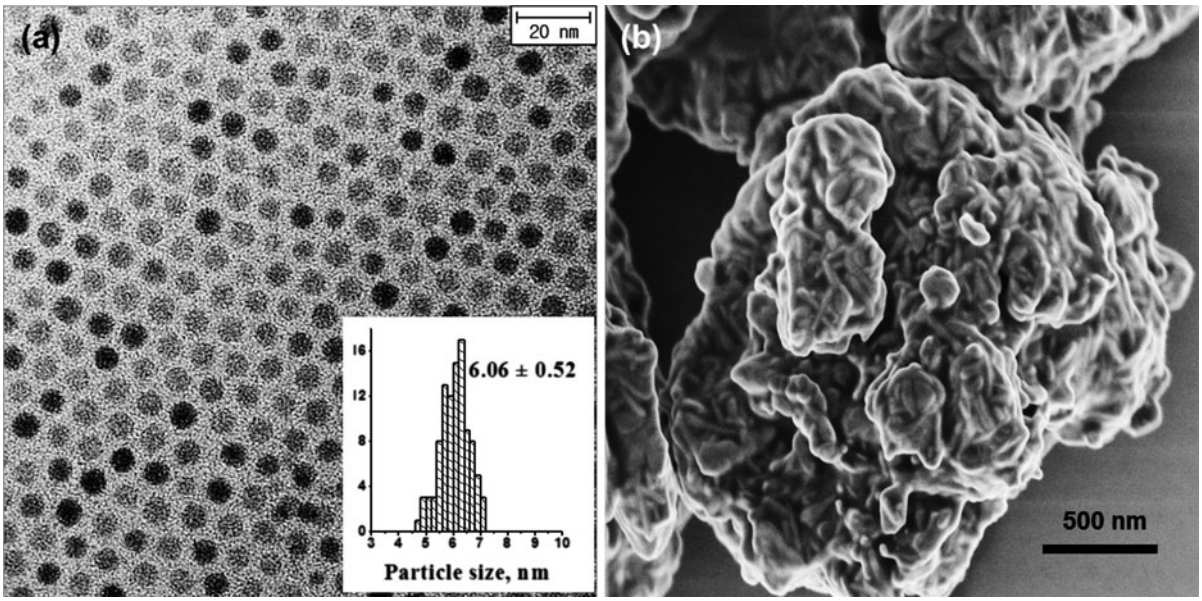

Fig. 2 **a** TEM image and particle size distribution of BHF, and **b** SEM image of annealed BHF-750

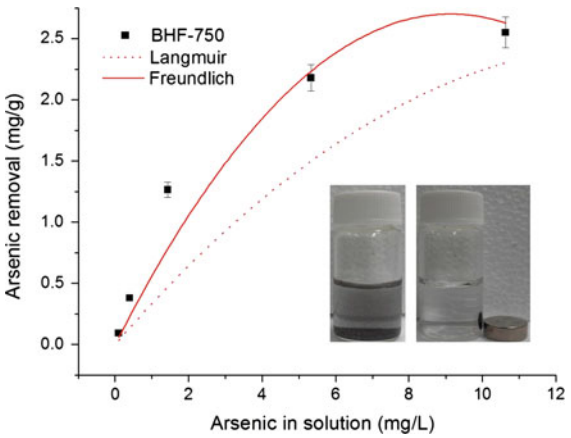

Fig. 3 Arsenic adsorption studies with nanocrystalline BHF-750 (*Inset* easy separation of BHF-750 from wastewater)

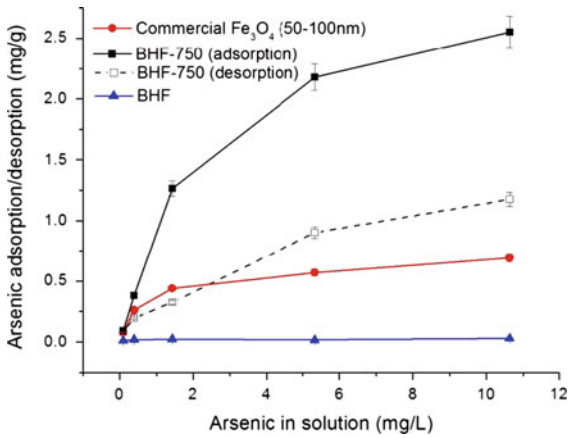

Fig. 4 Arsenic adsorption/desorption studies on BHF-750, arsenic adsorption studies on commercial Fe_3O_4 (50–100 nm) and uncalcined BHF

related to the adsorption capacity and intensity, respectively; and q_e (mg/g) is the mass of arsenic adsorbed per mass of adsorbent. Regression coefficients (r^2) for Langmuir and Freundlich isotherm is 0.92 and 0.96, indicating that both the models fit reasonably well with As(III) adsorption. The maximum monolayer adsorption capacity (q_m) obtained for BHF-750 is 2.27 mg/g which is comparable with experimental capacity of 2.55 mg/g. The Freundlich adsorption intensity parameters (n) is 3.8, also supporting the favorable adsorption of As(III) on BHF-750.

As(III) removal efficiency of BHF-750 is higher than the capacity of commercial magnetite, Fe_3O_4 (0.25 mg/g) of 300 nm size (Yavuz et al. 2006). Furthermore, commercial Fe_3O_4 (50–100 nm) and BHF (non-calcined sample) were also studied for As(III) removal under identical conditions as shown in Fig. 4. The As(III) removal capacity for commercial Fe_3O_4 and BHF is 0.7 and 0.03 mg/g. This behavior

Table 2 Recovery efficiencies of BHF-750 after As(III) adsorption tests

As(III) concentration (mg/L)	Initial dosage of BHF-750 (g)	Residual BHF (after treatment) (g)	%	Remarks
0.1	0.0098	0.0113	115	Residual BHF-750 was weighed after drying for 3 h at 90 °C
0.5	0.012	0.0098	82	
1	0.0099	0.0095	96	
5	0.01	0.014	140	
10	0.0098	0.0121	123	

suggests that hexaferrites of nanodimensional sized gave better arsenic removal efficiency than commercial Fe_3O_4 nanoparticles. The arsenic adsorption was reduced significantly at high pH and arsenic was desorbed from the magnetite at alkaline pH (Yean et al. 2005; Phu et al. 2009). After arsenic adsorption, BHF-750 were treated with alkaline solution of pH 13 for desorption of arsenic (Fig. 4). It was found that 55 % of the arsenic was desorbed from BHF-750.

Recovery of BHF-750 after arsenic removal was calculated by measuring post-treatment weight of magnetically separated adsorptive media (Table 2). The sorbents were dried for 3 h at 90 °C to make sure no water remained adsorbed. The recoveries were mostly found to exceed quantitative amounts, suggesting that adsorbed species tend to immobilize on the surface in the form of arsenites or hydroxylates.

Conclusions

In summary, we found that BHF nanoparticles offer better arsenic capacity and much versatile handling than their magnetite counterparts. This behavior proves useful when the removal of arsenic by magnetic nanoparticles are taken to the actual field operations. However, it is found to be difficult to form barium hexaferrite hexagonal phase at low temperatures. Only, the subsequent annealing at 750 °C of BHF nanoparticles synthesized by solvothermal method resulted hexagonal phase. Size control and monodispersity of BHF nanoparticles are lost after annealing, as expected. Arsenic removal efficiency of annealed BHF (BHF-750) is 75 % which is quite higher than magnetite nanoparticles of similar size. This proves that metal hexaferrites are potential materials for heavy metal removal application from wastewater. Moreover, hard magnetic behavior of metal hexaferrites may solve the problem of separation of treated nanoparticles from water at low magnetic field. When attempted to recycle the adsorbent, it was found that 55 % of the arsenic was desorbed from BHF-750 in aqueous alkaline solution.

Acknowledgments This study is supported by KAIST EEWS Initiative 2011–2013 for the development of enhanced water treatment technologies by nanoscale ferrites and their carbon assemblies. This work was also supported by the National Research Foundation of Korea Grant funded by the Korean Government (MEST) (NRF-2012-C1AAA001-M1A2A2026588).

References

Acharyya SK, Chatraborty P, Lahiri S, Raymahashay BC, Guha S, Bhowmik A (1999) Arsenic poisoning in the Ganges delta. Nature 401:545–546

Bao N, Shen L, Wang Y, Padhan P, Gupta A (2007) A facile thermolysis route to monodisperse ferrite nanocrystals. J Am Chem Soc 129:12374–12375

Beker U, Cumbal L, Duranoglu D, Kucuk I, Sengupta AK (2010) Preparation of Fe oxide nanoparticles for environmental applications: arsenic removal. Environ Geochem Health 32:291–296

Bhakat PB, Gupta AK, Ayoob S, Kundu S (2006) Investigations on arsenic(V) removal by modified calcined bauxite. Colloids Surf A 281:237–245

Biswas BK, Inoue J, Inoue K, Ghimire KN, Harada H, Ohto K, Kawakita H (2008) Adsorptive removal of As(V) and As(III) from water by a Zr(IV)-loaded orange waste gel. J Hazard Mater 154:1066–1074

Borah D, Satokawa S, Kato S, Kojima T (2009) Sorption of As(V) from aqueous solution using acid modified carbon black. J Hazard Mater 162:1269–1277

Cumbal L, Greenleaf J, Leun D, SenGupta AK (2003) Polymer supported inorganic nanoparticles: characterization and environmental applications. React Funct Polym 54:167–180

Hessien MM, Rashad MM, El-Barawy K (2008) Controlling the composition and magnetic properties of strontium hexaferrite synthesized by co-precipitation method. J Magn Magn Mater 320:336–343

Hyeon T, Chung Y, Park J, Lee SS, Kim Y-W, Park BH (2002) Synthesis of highly crystalline and monodisperse cobalt ferrite nanocrystals. J Phys Chem B 106:6831–6833

Junliang L, Yanwei Z, Cuijing G, Wei Z, Xiaowei Y (2010) One-step synthesis of barium hexaferrite nano-powders via microwave-assisted sol–gel auto-combustion. J Eur Ceram Soc 30:993–997

Kwon SG, Hyeon T (2008) Colloidal chemical synthesis and formation kinetics of uniformly sized nanocrystals of metals, oxides, and chalcogenides. Acc Chem Res 41(12):1696–1709

Li Z, Beachner R, McManama Z, Hanlie H (2007) Sorption of arsenic by surfactant-modified zeolite and kaolinite. Microporous Mesoporous Mater 105:291–297

Lim S-F, Zheng Y-M, Paul Chen J (2009) Organic arsenic adsorption onto a magnetic sorbent. Langmuir 25(9):4973–4978

Mayo JT, Yavuz C, Yean S, Cong L, Shipley H, Yu W, Falkner J, Kan A, Tomson M, Colvin VL (2007) The effect of nanocrystalline magnetite size on arsenic removal. Sci Technol Adv Mater 8:71–75

Mohan D, Pittman CU Jr (2007) Arsenic removal from water/wastewater using adsorbents—a critical review. J Hazard Mater 142(1–2):1–53

Patel HA, Bajaj HC, Jasra RV (2008) Synthesis of Pd and Rh metal nanoparticles in the interlayer space of organically modified montmorillonite. J Nanopart Res 10:625–632

Pena ME, Korfiatis GP, Patel M, Lippincott L, Meng X (2005) Adsorption of As(V) and As(III) by nanocrystalline, Titanium dioxide. Water Res 39:2327–2337

Phu ND, Phong PC, Chau N, Luong NH, Hoang LH, Hai NH (2009) Arsenic removal from water by magnetic $Fe_{1-x}Co_xFe_2O_4$ and $Fe_{1-y}Ni_yFe_2O_4$ nanoparticles. J Exp Nanosci 4(3):253–258

Ranjan D, Talat M, Hasan SH (2009) Biosorption of arsenic from aqueous solution using agricultural residue 'rice polish'. J Hazard Mater 166:1050–1059

Sharma VK, Sohn M (2009) Aquatic arsenic: toxicity, speciation, transformations, and remediation. Environ Int 35:743–759

Shipley HJ, Engates KE, Guettner AM (2011) Study of iron oxide nanoparticles in soil for remediation of arsenic. J Nanopart Res 13:2387–2397

Tang W, Li Q, Li C, Gao S, Shang JK (2011) Ultrafine α-Fe_2O_3 nanoparticles grown in confinement of in situ self-formed ''cage'' and their superior adsorption performance on arsenic(III). J Nanopart Res 13:2641–2651

Tucek J, Zboril R, Namai A, Ohkoshi S (2010) ε-Fe_2O_3: an advanced nanomaterial exhibiting giant coercive field, millimeter-wave ferromagnetic resonance, and magnetoelectric coupling. Chem Mater 22:6483–6505

Yavuz CT, Mayo JT, Yu WW, Prakash A, Falkner JC, Yean S, Cong L, Shipley HJ, Kan A, Tomson M, Natelson D, Colvin VL (2006) Low-field magnetic separation of monodisperse Fe_3O_4 nanocrystals. Science 314:964–967

Yavuz CT, Prakash A, Mayo JT, Colvin VL (2009) Magnetic separations: from steel plants to biotechnology. Chem Eng Sci 64:2510–2521

Yavuz CT, Mayo JT, Suchecki C, Wang J, Ellsworth AZ, D'Couto H, Quevedo E, Prakash A, Gonzalez L, Nguyen C, Kelty C, Colvin VL (2010) Pollution magnet: nanomagnetite for arsenic removal from drinking water. Environ Geochem Health 32:327–334

Yean S, Cong L, Yavuz CT, Mayo JT, Yu WW, Colvin VL, Tomson MB (2005) Effect of magnetite particle size on adsorption and desorption of arsenite and arsenate. J Mater Res 20(12):3255–3264

Zeng H, Li J, Liu JP, Wang ZL, Sun S (2002) Exchange-coupled nanocomposite magnets by nanoparticles self-assembly. Nature 420:395–398

Zhao X, Wang J, Wub F, Wang T, Cai Y, Shi Y, Jiang G (2010) Removal of fluoride from aqueous media by Fe_3O_4@Al$(OH)_3$ magnetic nanoparticles. J Hazard Mater 173:102–109

Zhao X, Guo X, Yang Z, Liu H, Qian Q (2011) Phase-controlled preparation of iron (oxyhydr)oxide nanocrystallines for heavy metal removal. J Nanopart Res 13:2853–2864